Enzyme Activities of the Ceramide Synthases CERS2– 6 Are Regulated by Phosphorylation in the C-terminal Region*

Takayuki Sassa, Taisuke Hirayama, and Akio Kihara[1]

From the Laboratory of Biochemistry, Faculty of Pharmaceutical Sciences, Hokkaido University, Kita-ku, Sapporo 060-0812, Japan

Ceramide and complex sphingolipids regulate important cellular functions including cell growth, apoptosis, and signaling. Dysregulation of sphingolipid metabolism leads to pathological consequences such as sphingolipidoses and insulin resistance. Ceramides in mammals vary greatly in their acyl-chain composition: six different ceramide synthase isozymes (CERS1– 6) that exhibit distinct substrate specificity and tissue distribution account for this diversity. In the present study, we demonstrated that CERS2– 6 were phosphorylated at the cytoplasmic C-terminal regions. Most of the phosphorylated residues conformed to a consensus motif for phosphorylation by casein kinase 2 (CK2), and treatment of cells with the CK2-specific inhibitor CX-4945 lowered the phosphorylation levels of CERS2, -4, -5, and -6. Phosphorylation of CERS2 was especially important for its catalytic activity, acting mainly by increasing its V_{max} value. Phosphorylation modestly increased the catalytic activities of CERS4 and -5 and mildly increased those of CERS3 and -6. Dephosphorylation of endogenous ceramide synthases in the mouse brain led to severely reduced activity toward the Cers2 substrates C22:0/C24:0-CoAs and modestly reduced activity toward the Cers5/6 substrate C16:0-CoA. These results suggest that the phosphorylation of ceramide synthases may be a key regulatory point in the control of the distribution and levels of sphingolipids of various acyl-chain lengths.

Sphingolipids, one of the major lipid constituents of eukaryotic membranes, mediate a number of cellular and physiological functions such as cell growth, apoptosis, immune responses, and the epidermal permeability barrier, whereas their abnormal metabolism is involved in diseases such as sphingolipidoses, neural disorders, and diabetes (1–7). Ceramides are located in the hub of sphingolipid metabolism. Ceramides are precursors for complex sphingolipids, whereas their hydrolysis releases a sphingoid long-chain base and a fatty acid (FA).[2] The released long-chain base can then be recycled to synthesize new ceramide, or metabolized further into other lipids such as sphingosine 1-phosphate (8 –10). Ceramide synthases catalyze the formation of an amide bond between the long-chain base and the FA in the endoplasmic reticulum. In most tissues, the chain lengths of the FA moieties of ceramides are C16 –C24, whereas the ceramides of skin and testis are exceptional in that they contain FAs with up to C36 (11–13). FAs can be classified by chain length: long-chain (LC) FAs have C11-C20, very-long-chain (VLC) FAs have ≥C21, and ultra long-chain (ULC) FAs have ≥C26 (11, 12). There are six mammalian ceramide synthase isozymes (human CERS1– 6 and mouse Cers1– 6) that exhibit distinct specificity for acyl-CoAs of defined chain lengths (9, 14 –16). Thus, the expression levels of ceramide synthase isozymes largely determine the levels and acyl-chain compositions of the ceramides present within a cell type or tissue.

The functional importance of ceramides and sphingolipids with defined acyl-chain lengths has been revealed by a number of studies. LC-ceramide, especially C16-ceramide, is generally pro-apoptotic, whereas VLC C24:0/C24:1-ceramides are anti-apoptotic (17, 18). During cytokinesis, the levels of C22- and C24-ceramides are increased, and these VLC-ceramides are accumulated in the midbody (19). Knockdown of *CERS2* or *CERS4*, which synthesize VLC-ceramides, results in cytokinesis failure (19). In the adipose tissue of obese humans, *CERS6* mRNA expression and C16-ceramide are elevated, and increased *CERS6* expression correlates with insulin resistance (6). Conversely, *Cers6*-deficient mice are protected from high fat diet-induced obesity and glucose intolerance (6). CERS1, which is important for the synthesis of C18-ceramide and predominantly expressed in the brain and skeletal muscle, is mutated in a form of myoclonic epilepsy (7). *Cers1*-deficient mice exhibit cerebellar abnormalities and behavioral deficits including in motor coordination (20, 21). ULC-ceramides are synthesized by CERS3 (22), and *CERS3/Cers3* deficiency in humans and mice leads to epidermal permeability barrier defects through the resulting reduction in ULC-ceramide levels (22, 23). Moreover, Cers3-dependent formation of ULC-ceramides is essential for spermatogenesis and fertility in mice (24). These data highlight the independent role of each ceramide synthase isozyme and implicate ceramide synthases as novel targets for therapeutic interventions for diseases in which sphingolipids with particular acyl-chain lengths are pathogenically involved (5, 16).

The regulation of ceramide synthase activity is poorly understood. What is known is that ceramide synthases can exist as complexes, and homo- or heterodimerization modulates CERS

[1] To whom correspondence should be addressed. Tel.: 81-11-706-3754; Fax: 81-11-706-4900; E-mail: kihara@pharm.hokudai.ac.jp.
[2] The abbreviations used are: FA, fatty acid; LC, long-chain; VLC, very long-chain; ULC, ultra long-chain; TORC2, target of rapamycin complex 2; CK2, casein kinase 2; MT, mutant; λPPase, λ protein phosphatase; PNGase F, protein *N*-glycosidase F.

activity (25). Ceramide synthases are subject to post-translational modifications including glycosylation and phosphorylation. CERS2, -5, and -6 can be *N*-glycosylated at the N-terminal region, although the glycosylation is dispensable for CERS6 activity (14). Global analysis of protein phosphorylation sites by MS has identified that CERS2 and -5 are phosphorylated at multiple residues in the C-terminal regions (26).

What remains to be demonstrated is whether the phosphorylation of ceramide synthases actually modulates their enzymatic activities. In this line of research, it has recently been demonstrated that Lac1 and Lag1, the CERS homologs of yeast *Saccharomyces cerevisiae*, are phosphorylated by two protein kinases, Ypk1 and Cka2 (27, 28). Ypk1, which is activated by the target of rapamycin complex 2 (TORC2), phosphorylates two serine residues at the N-terminal regions of Lac1 and Lag1 and increases their synthetic activities (28). Cka2 is the catalytic subunit of casein kinase 2 (CK2) and phosphorylates three serine residues at the C-terminal regions of Lac1 and Lag1 (27). The Cka2-dependent phosphorylation of Lac1 and Lag1 is required for efficient ceramide biosynthesis (27). These results raised an important question in the field of sphingolipid metabolism: are the activities of mammalian ceramide synthases also regulated by phosphorylation?

In the present study, we examined whether six mammalian ceramide synthase isozymes are phosphorylated. We found that CERS2–6 were phosphorylated in the C-terminal regions and determined their phosphorylation sites. We also demonstrated that the enzymatic activity of CERS2 is heavily dependent on phosphorylation, whereas those of CERS3–6 are modestly or mildly increased by it. Finally, we revealed that the phosphorylation of CERS2 increases its V_{max} value and modulates its affinities toward sphingosine and acyl-CoA, but in opposite directions.

Experimental Procedures

Cell Culture and Transfection—HEK 293T cells were grown in DMEM (D6429; Sigma) containing 10% fetal bovine serum and supplemented with 100 units/ml of penicillin and 100 μg/ml of streptomycin. Cells were seeded in dishes coated with 0.3% collagen and maintained in a humidified atmosphere of 5% CO_2 at 37 °C. Transfections were performed using Lipofectamine Plus Reagent (Thermo Fisher Scientific, Waltham, MA) according to the manufacturer's instructions.

Plasmid Construction—Plasmids and primers used in this study are listed in Tables 1 and 2, respectively. Human *CERS1*, *-5*, and *-6* cDNAs were amplified by PCR using human tissue cDNAs (Human MTC panels I; TAKARA Bio, Shiga, Japan) as templates (for *CERS1*, pancreas cDNA; for *CERS5*, skeletal muscle cDNA; for *CERS6*, kidney cDNA) and primers (for *CERS1*, CERS1-F1 and CERS1-R1; for *CERS5*, CERS5-F1 and CERS5-R1; for *CERS6*, CERS6-F1 and CERS6-R1). Mouse *Cers2* cDNA was amplified by PCR using the pcDNA3 HA-Cers2 plasmid (14) as a template and primers Cers2-F1 and Cers2-R1. Each amplified DNA fragment was cloned into the pGEM-T Easy vector (Promega, Fitchburg, WI). Human *CERS2*, *CERS3*, and *CERS4* cDNAs cloned into the pGEM-T Easy vector have been described previously (29, 30). Human *CERS2 (S341A/T346A/S348A/S349A)* abbreviated as *CERS2*

TABLE 1
Plasmids used in this study
All inserts are cloned into the mammalian expression vector pCE-puro HA-1, which is designed to produce a protein fused to an N-terminal HA tag.

Plasmid	Insert	Species
pHT46	*CERS1*	Human
pHT56	*CERS2*	Human
pHT57	*CERS2 (4A)*	Human
pHT50	*CERS3*	Human
pHT51	*CERS3 (S340A)*	Human
pHT52	*CERS4*	Human
pHT53	*CERS4 (4A)*	Human
pHT58	*CERS5*	Human
pHT59	*CERS5 (4A)*	Human
pHT54	*CERS6*	Human
pHT55	*CERS6 (4A)*	Human
pHT35	*Cers2*	Mouse
pHT42	*Cers2 (S341A)*	Mouse
pHT45	*Cers2 (T346A)*	Mouse
pHT43	*Cers2 (S348A)*	Mouse
pHT44	*Cers2 (S349A)*	Mouse
pHT33	*Cers2 (4A)*	Mouse

(4A), *CERS3 (S340A)*, *CERS4 (S343A/S348A/S350A/S351A)* abbreviated as *CERS4 (4A)*, *CERS5 (S350A/S354A/S355A/S356A)* abbreviated as *CERS5 (4A)*, *CERS6 (S341A/S345A/S346A/S347A)* abbreviated as *CERS6 (4A)*, mouse *Cers2 (S341A)*, *Cers2 (T346A)*, *Cers2 (S348A)*, *Cers2 (S349A)*, and *Cers2 (S341A/T346A/S348A/S349A)* abbreviated as *Cers2 (4A)* (Table 1) were constructed using the overlap extension PCR (for mutant (MT) forms of human *CERS2– 6*) or QuikChange site-directed mutagenesis kit (Agilent Technologies, Santa Clara, CA) (for MTs of mouse *Cers2*), with appropriate WT plasmid as a template and primers (for *CERS2 (4A)*, CERS2– 4A-F and CERS2– 4A-R; for *CERS3 (S340A)*, CERS3-S340A-F and CERS3-S340A-R; for *CERS4 (4A)*, CERS4 – 4A-F and CERS4 – 4A-R; for *CERS5 (4A)*, CERS5 – 4A-F and CERS5– 4A-R; for *CERS6 (4A)*, CERS6 – 4A-F and CERS6 – 4A-R; for *Cers2 (S341A)*, Cers2-S341-F and Cers2-S341-R; for *Cers2 (T346A)*, Cers2-T346-F and Cers2-T346-R; for *Cers2 (S348A)*, Cers2-S348-F and Cers2-S348-R; for *Cers2 (S349A)*, Cers2-S349-F and Cers2-S349-R; for *Cers2 (4A)*, Cers2– 4A-F and Cers2– 4A-R) (Table 2). Each cDNA fragment was excised from the corresponding pGEM-T Easy-based plasmid and cloned into a mammalian expression vector pCE-puro HA-1, which is designed to produce a protein fused to an N-terminal HA tag under control of the human elongation factor 1α promoter (31).

Immunoblotting—Immunoblotting was performed as described previously (32) using the anti-HA antibody HA-7 (1:2,000 dilution; Sigma) as the primary antibody and HRP-conjugated anti-mouse IgG F(ab′)$_2$ fragment (1:7,500 dilution; GE Healthcare Life Sciences, Little Chalfont, UK) as the secondary antibody. The signal was detected with Pierce Western blotting Substrate (Thermo Fisher Scientific) or Western Lightning Plus-ECL (PerkinElmer Life Sciences).

Preparation of Membrane Fractions—The membrane fraction of HEK 293T cells was prepared as follows. Cells were suspended in buffer A (50 mM HEPES-NaOH (pH 7.4), 150 mM NaCl, 10% glycerol, 1 mM DTT, 1 mM PMSF, and a 1× Complete protease inhibitor mixture (EDTA-free; Roche Diagnostics, Basel, Switzerland)) and lysed by sonication; cell debris was removed by centrifugation at 300 × *g* and 4 °C for 5 min; the supernatant was centrifuged at 100,000 × *g* and 4 °C for 30 min;

TABLE 2
Nucleotide sequences of primers used in this study
The restriction sites created are underlined.

Primer	Nucleotide sequence
CERS1-F1	5′-<u>GGGATCC</u>ATGGCGGCGGCGGGGCCCGCGGCGG-3′ (BamHI)
CERS1-R1	5′-TCAGAAGCGCTTGTCCTTCACCAGG-3′
CERS2–4A-F	5′-GCTGACCGGGAAGAAGCAGAGGCCGCAGAGGGGGAGGAGGCTGCAGCTGG-3′
CERS2–4A-R	5′-TGCGGCCTCTGCTTCTTCCCGGTCAGCGCGTTCATCTTCTACCAGCTTTC-3′
CERS3-S340A-F	5′-GAGCATCCAGATGGTGAGGGCTGATGCGGAGGATTATGAAGAGG-3′
CERS3-S340A-R	5′-CCTCTTCATAATCCTCGTCATCAGCCCTCACATCCTGGATGCTC-3′
CERS4–4A-F	5′-CCAGATGGAGAAGGACATTCGTGCTGATGTAGAAGAAGCAGACGCC-GCTGAGGAGGCGGCGGCGGCCCAGG-3′
CERS4–4A-R	5′-CCTGGGCCGCCGCCGCCTCCTCAGCGGCCGTCTGCTTCTTCTACATCA-GCACGAATGTCCTTCTCCATCTGG-3′
CERS5-F1	5′-<u>GGATCC</u>ATGGCGACAGCAGCGCAGGGACCCC-3′ (BamHI)
CERS5-R1	5′-TTACTCTTCAGCCCAGTAGCTGCCT-3′
CERS5–4A-F	5′-CGCTGATGTGGAGGCCGCCGCAGAGGAAGAAGATGTGACCACCTG-3′
CERS5–4A-R	5′-GCGGCGGCCTCCACATCAGCGCGATCATCCTTCGATACCTTTCCC-3′
CERS6-F1	5′-<u>GGATCC</u>ATGGCAGGGATCTTAGCCTGGTTCT-3′ (BamHI)
CERS6-R1	5′-TTAATCATCCATGGAGCAGGAGCCA-3′
CERS6–4A-F	5′-CATGTGTCCAAGGATGATCGAGCTGATATTGAGGCTGCCGCAGATG-AGGAGGACTCAGAACC-3′
CERS6–4A-R	5′-GGTTCTGAGTCCTCCTCATCTGCGGCAGCCTCAATATCAGCTCGATC-ATCCTTGGACACATG-3′
Cers2-F1	5′-<u>TGATCA</u>ATGCTCCAGACCTTGTATGACTACT-3′ (BclI)
Cers2-R1	5′-<u>GCGGCCGC</u>CTCAGTCATTCTTAGGATGATTGTTA-3′ (NotI)
Cers2-S341-F	5′-GCTGATAGAAGATGAACGCGCTGACAGAGAAGAAACAGAGAG-3′
Cers2-S341-R	5′-CTCTCTGTTTCTTCTCTGTCAGCGCGTTCATCTTCTATCAGC-3′
Cers2-T346-F	5′-CGCAGTGACAGAGAAGAAGCAGAGAGTTCAGAGGGGGAGG-3′
Cers2-T346-R	5′-CCTCCCCCTCTGAACTCTCTGCTTCTTCTCTGTCACTGCG-3′
Cers2-S348-F	5′-GCAGTGACAGAGAAGAAACAGAGGCATCAGAGGGGGAGGAGACTGC-3′
Cers2-S348-R	5′-GCAGTCTCCTCCCCCTCTGATGCCTCTGTTTCTTCTCTGTCACTGC-3′
Cers2-S349-F	5′-CAGAGAAGAAACAGAGAGTGCAGAGGGGGAGGAGACTGCAGC-3′
Cers2-S349-R	5′-GCTGCAGTCTCCTCCCCCTCTGCACTCTCTGTTTCTTCTCTG-3′
Cers2–4A-F	5′-GCTGATAGAAGATGAACGCGCTGACAGAGAAGAAGCAGAGGCAGC-AGAGGGGGAGGAGACTGCAGC-3′
Cers2–4A-R	5′-GCTGCAGTCTCCTCCCCCTCTGCTGCCTCTGCTTCTTCTCTGTCAGCG-CGTTCATCTTCTATCAGC-3′

and the pellet (total membrane fraction) was suspended in buffer A. Treatment with λ protein phosphatase (λPPase) (New England Biolabs, Ipswich, MA) and protein *N*-glycosidase F (PNGase F) (New England Biolabs) were performed by incubating the membrane with λPPase (8 units/μg of membrane protein) and PNGase F (20 units/μg of membrane protein) in protein metallophosphatases buffer (50 mM HEPES (pH 7.5), 100 mM NaCl, 2 mM DTT, 0.01% Brij 35, and 0.1 mM $MnCl_2$; New England Biolabs) at 30 °C for 60 min.

In Vitro Ceramide Synthase Assay—The ceramide synthase assay was performed by incubating the membrane fraction with 5 μM deuterium-labeled sphingosine (sphingosine-d_7; Avanti Polar Lipids, Alabaster, AL) and 25 μM acyl-CoA in 100 μl of reaction buffer (buffer A containing 2 mM $MgCl_2$ and 0.1% digitonin) at 37 °C for 30 min. Kinetic analysis of WT HA-CERS2 was performed by changing the concentrations of one substrate, while fixing the concentration of the other at 5 and 25 μM for sphingosine-d_7 and C24:1-CoA, respectively. C16:0 (palmitoyl)-CoA, C18:0 (stearoyl)-CoA, and C20:0 (arachidoyl)-CoA were purchased from Sigma, whereas C24:0 (lignoceroyl)-CoA and C24:1 (nervonoyl)-CoA were purchased from Avanti Polar Lipids. The reaction was terminated by the addition of 375 μl of chloroform/methanol (1:2, v/v) and 1.25 μl of 12 M formic acid, followed by vigorous shaking. The mixture was subjected to phase separation by adding 125 μl of chloroform and 125 μl of H_2O, followed by centrifugation (9,000 × *g*, room temperature, 3 min). Lipids were recovered from the organic phase, dried, and suspended in chloroform/methanol (1:2, v/v). Deuterium-labeled ceramide (ceramide-d_7) species were detected by LC/MS (see below).

Lipid Analysis Using LC/MS—Ceramides were analyzed by reversed-phase LC/MS using ultra-performance liquid chromatography coupled with electrospray ionization tandem triple quadrupole MS (Xevo TQ-S, Waters, Milford, MA) as described previously (29). Each ceramide species was detected by multiple reaction monitoring by selecting the *m/z* ([M-H_2O + H]$^+$ and [M + H]$^+$) of specific ceramide species at Q1 and the *m/z* 264.2 for ceramide and the *m/z* 271.2 for ceramide-d_7, respectively, at Q3 (Table 3). Data analysis and quantification were performed using MassLynx software (version 4.1; Waters).

Results

CERS2– 6 Proteins Are Phosphorylated Mainly at the C-terminal Region—Mammalian CERS1– 6 are multispanning membrane proteins with five predicted transmembrane segments (Fig. 1). Examination of the amino acid sequences of the CERS1– 6 C-terminal regions revealed the presence of potential phosphorylation sites in CERS2– 6 (Fig. 1). They are mostly conserved between human CERS2– 6 and the corresponding mouse Cers2– 6 proteins, and bear resemblance to the phosphorylation sites in yeast *S. cerevisiae* ceramide synthases Lac1 and Lag1 (27) (Fig. 1). Most of the potentially phosphorylated serine residues match the consensus motif for phosphorylation by CK2 (*i.e.* (S/T)*XX*(D/E), where *X* stands for any amino acid, S for serine, T for threonine, D for aspartate, and E for glutamate) (33) (Fig. 1). Proteome analysis of phosphorylation sites by MS has previously identified that four residues in CERS2 (Ser-341, Thr-346, Ser-348, and Ser-349) and CERS5 (Ser-350, Ser-354, Ser-355, and Ser-356) are phosphorylated in HeLa

TABLE 3
Selected *m/z* values for ceramide species in MS analysis

Cer[a] species	Precursor ion (Q1)	Product ion (Q3)	Collision energy (in V)
d18:1/C16:0 Cer	520.2, 538.2	264.2	20
d18:1/C16:0 Cer-d_7	527.2, 545.2	271.2	20
d18:1/C18:0 Cer	548.2, 566.2	264.2	20
d18:1/C18:0 Cer-d_7	555.2, 573.2	271.2	20
d18:1/C20:0 Cer	576.3, 594.3	264.2	25
d18:1/C20:0 Cer-d_7	583.3, 601.3	271.2	25
d18:1/C22:1 Cer	602.3, 620.3	264.2	25
d18:1/C22:0 Cer	604.3, 622.3	264.2	25
d18:1/C24:1 Cer	630.3, 648.3	264.2	30
d18:1/C24:1 Cer-d_7	637.3, 655.3	271.2	30
d18:1/C24:0 Cer	632.3, 650.3	264.2	30
d18:1/C24:0 Cer-d_7	639.3, 657.3	271.2	30
d18:1/C26:0 Cer	660.4, 678.4	264.2	30

[a] Cer, ceramide; Cer-d_7, deuterium-labeled ceramide.


```
human CERS1 313 QVHELKDLREYDTAEAQSLKPSKA 336
mouse Cers1 313 QMRELEDLREYDTLEAQTAKPCKA 336

human CERS2 334 KLVEDERSDREETESSEGEEAAAG 357
mouse Cers2 334 KLIEDERSDREETESSEGEETAAG 357

human CERS3 333 KSIQDVRSDDEDYEEEEEEEEEA 356
mouse Cers3 369 QNVQDVRSDNEEEEEEEEEEEAES 392

human CERS4 336 QMEKKIRSDVEESDSSEEAAAAQE 359
mouse Cers4 335 QMTEDIRSDVEEPDSSDDEPVSEG 358

human CERS5 343 KVSKDDRSDVESSSEEEDVTTCTK 366
mouse Cers5 343 KVSKDDRSDVESSSEEEDETTHKN 366

human CERS6 334 KVSKDDRSDIESSSDEEDSEPPGK 357
mouse Cers6 334 KVSKDDRSDIESSSDDEDSEPPGK 357

yeast Lac1 386 GILKDDRSDSESDEESDESSTTPT 409
yeast Lag1 386 GIQKDERSDSDSDESAENEESKEK 409
```
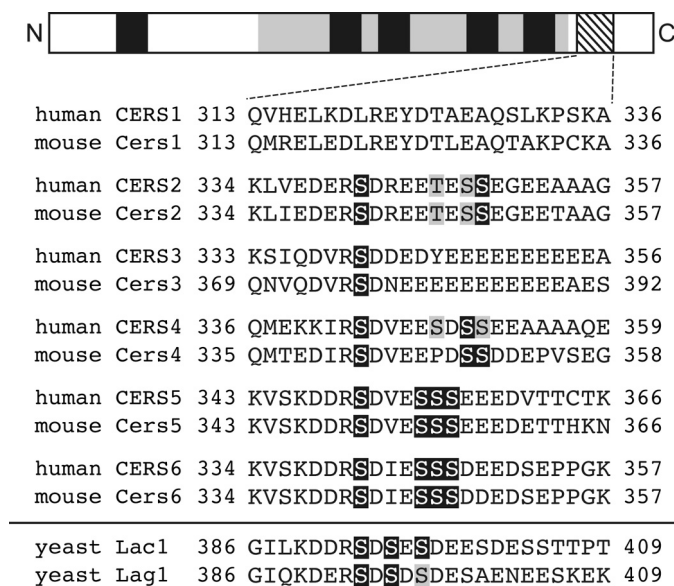
FIGURE 1. Potential phosphorylation sites in the C-terminal regions of CERS2–6. The schematic illustration of mammalian CERS1–6 denotes the five predicted transmembrane segments and the TRAM/LAG1/CLN8 (TLC) homology domain (45), shown as *black* and *gray regions*, respectively. The region around the potential phosphorylation sites is *shaded*, and the amino acid sequences of human CERS1–6 and mouse Cers1–6 in the region are presented below it. Amino acid residues analyzed in this study are highlighted in *black* or *gray boxes*, with the former denoting CK2 phosphorylation sites. For comparison, amino acid sequences and phosphorylation sites in the C-terminal region of yeast Lac1 and Lag1 are presented (27).

cells (26). To examine whether CERS1–6 are phosphorylated, we expressed the N terminally HA-tagged versions of WT CERS1–6 (HA-CERS1–6) in HEK 293T cells and treated the total membrane fractions with λPPase only, PNGase F only, and a combination of the two. We examined the electrophoretic mobility of each HA-CERS protein by SDS-PAGE, followed by immunoblotting. WT HA-CERS1 was detected as a single band, and its mobility did not shift appreciably after treatment with λPPase or PNGase F, suggesting that HA-CERS1 was not phosphorylated or glycosylated (Fig. 2). Untreated WT HA-CERS2 was detected as three bands (Fig. 2). Treatment with λPPase increased the mobility of the top and middle bands, with the middle band merging with the bottom band. Treatment with PNGase F increased the mobility of the top band, which merged with the middle band. Treatment with both enzymes resulted in merging of the top and middle bands with

the bottom band. Thus, HA-CERS2 was phosphorylated and glycosylated, with the bottom band corresponding to the unmodified form of HA-CERS2, the middle band to the phosphorylated form, and the top band to the phosphorylated and glycosylated form. Untreated WT HA-CERS3 was detected as a single band, and treatment with λPPase resulted in a subtle but reproducible mobility shift, suggesting that HA-CERS3 was phosphorylated at only one or a few sites (Fig. 2). The mobility patterns of WT HA-CERS4–6 were essentially similar to those of HA-CERS2, except that their levels of the unmodified form were very low (Fig. 2). In summary, HA-CERS2–6 were phosphorylated, and HA-CERS2, -4, -5, and -6 were also glycosylated.

We next examined whether the observed phosphorylation is located at the potential phosphorylation sites in the C-terminal regions of CERS2–6 that were identified during the global phosphoproteomic analysis referred to in the above paragraph (26). We expressed the MT forms of HA-CERS2–6, in which the potential phosphorylation sites in the C-terminal region of each CERS (CERS2, Ser-341/Thr-346/Ser-348/Ser-349; CERS3, Ser-340; CERS4, Ser-343/Ser-348/Ser-350/Ser-351; CERS5, Ser-350/Ser-354/Ser-355/Ser-356; CERS6, Ser-341/Ser-345/Ser-346/Ser-347) were all substituted with Ala residues, and compared their electrophoretic mobilities with those of the corresponding WT proteins. Untreated MT HA-CERS2–6 showed essentially identical mobility patterns to those of λPPase-treated WT proteins (Fig. 2). Moreover, the treatment of MT HA-CERS2–6 with λPPase did not result in any further mobility shifts (Fig. 2). MT HA-CERS2, -4, -5, and -6 were glycosylated similarly to their corresponding WT proteins (Fig. 2). Taken together, these results demonstrate that HA-CERS2–6 are phosphorylated, and the major phosphorylation sites are located in the C-terminal region, although the possibility that additional phosphorylation sites are present cannot be excluded.

CK2 Phosphorylates CERS2, -4, -5, and -6 Proteins—As indicated before, CERS2–6 contain one to four putative CK2 phosphorylation sites in their C-terminal regions. To validate the sites, we treated cells expressing WT HA-CERS1–6 with CX-4945, a selective CK2 inhibitor currently in phase I and II clinical trials for cancer treatment (34–36), and examined the mobility of each HA-CERS protein by SDS-PAGE followed by immunoblotting. As expected, HA-CERS1 showed no mobility shift after CX-4945 treatment (Fig. 3). For HA-CERS2, which contains two potential CK2 phosphorylation sites, CX-4945 treatment caused a clear reduction in the phosphoHA-CERS2/HA-CERS2 ratio without an appreciable shift in the mobility of any form (Fig. 3). HA-CERS3 showed no mobility shift after CX-4945 treatment (Fig. 3). This result despite CERS3 containing one potential CK2 phosphorylation site (Ser-340) suggests this residue was likely phosphorylated by another kinase. The mobility of HA-CERS4–6 (possessing two or four potential CK2 phosphorylation sites each) shifted clearly after CX-4945 treatment toward the position of their corresponding MT proteins (Fig. 3). These results demonstrate that HA-CERS2, -4, -5, and -6 are substrates of CK2, and suggest that the CK2-dependent phosphorylation of CERS may be an evolutionarily con-
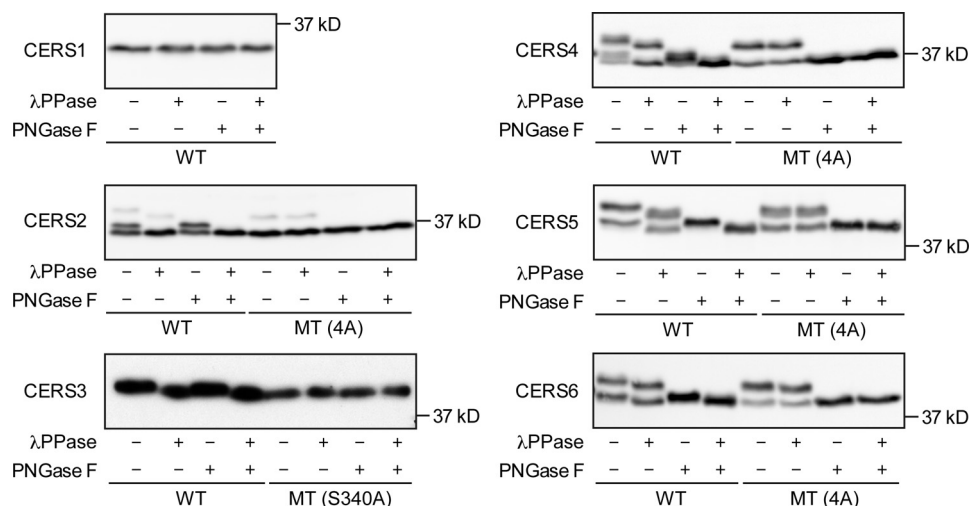
FIGURE 2. **CERS2–6 are phosphorylated.** HEK 293T cells were transfected with a plasmid encoding WT HA-CERS1–6 or MT HA-CERS2–6, as indicated. Total membrane fractions prepared from the transfected cells were treated with or without λPPase and PNGase F as indicated, separated by SDS-PAGE, and subjected to immunoblotting with anti-HA antibodies.
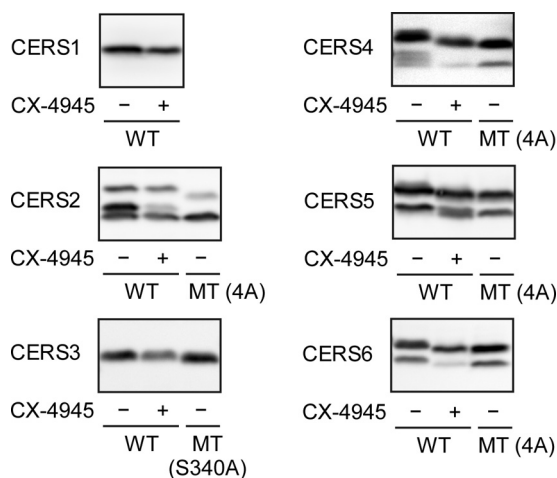

FIGURE 3. **CK2 phosphorylates CERS2, -4, -5, and -6.** HEK 293T cells were transfected with a plasmid encoding WT HA-CERS1–6 or MT HA-CERS2–6, as indicated. Three hours after transfection, the cells were incubated with or without 5 μM CK2 inhibitor CX-4945 at 37 °C for 21 h. Total lysates (20 μg of protein) prepared from the transfected cells were separated by SDS-PAGE and subjected to immunoblotting with anti-HA antibodies.
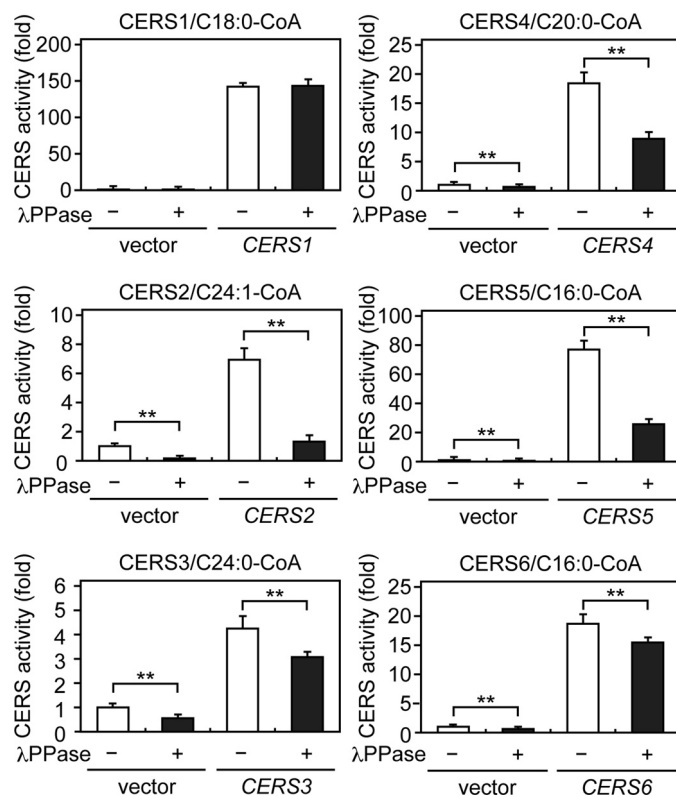

FIGURE 4. **CERS2 enzymatic activity is highly dependent on phosphorylation.** HEK 293T cells were transfected with a vector or a plasmid encoding HA-CERS1–6. Total membrane fractions (10 μg of protein) prepared from the transfected cells were treated with or without λPPase at 30 °C for 1 h, followed by incubation with 5 μM deuterium-labeled sphingosine and 25 μM of the indicated acyl-CoA at 37 °C for 30 min. Lipids were extracted, and deuterium-labeled ceramides were analyzed by a Xevo TQ-S LC/MS system and quantified by MassLynx software. The values represent the activity of each CERS relative to that of the vector/λPPase (−) sample and are the mean ± S.D. from three independent assays. Statistically significant differences are indicated; **, $p < 0.01$; t test.

served regulatory mechanism for the control of ceramide synthesis.

CERS2 Phosphorylation Is Important for Enzymatic Activity—We performed an *in vitro* ceramide synthase assay to examine the impact of phosphorylation on the enzymatic activity of the CERS isozymes. Membrane fractions prepared from HEK 293T cells expressing each HA-CERS protein were treated with or without λPPase, followed by incubation with acyl-CoA and deuterium-labeled sphingosine, and the levels of deuterium-labeled ceramide produced were determined using LC/MS. Treatment with λPPase significantly reduced the activities of HA-CERS2–6 to various degrees compared with untreated controls (Fig. 4). The activity of HA-CERS2 was most severely reduced (by 81%), whereas those of HA-CERS4 and -5 were modestly reduced (by 52 and 67%, respectively), and those of HA-CERS3 and -6 were mildly reduced (by 28 and 17%, respectively) (Fig. 4). In contrast, the activity of HA-CERS1 was not affected by λPPase treatment (Fig. 4). We noticed that the activ-

ities toward C16:0-, C20:0-, C24:0-, and C24:1-CoA in vector-transfected samples corresponding to those of endogenous CERS proteins were also significantly reduced by λPPase treatment compared with untreated controls (Fig. 4). The most
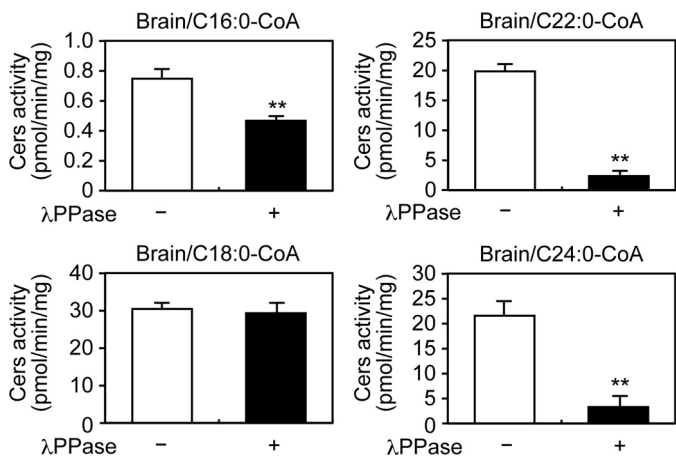
FIGURE 5. **Phosphorylation positively regulates the enzymatic activities of endogenous ceramide synthases in the brain.** Total membrane fractions (30 μg of protein) prepared from mouse brain were treated with or without λPPase at 30 °C for 1 h, followed by incubation with 5 μM deuterium-labeled sphingosine and 25 μM of the indicated acyl-CoA at 37 °C for 30 min. Lipids were extracted, and deuterium-labeled ceramides were analyzed by a Xevo TQ-S LC/MS system and quantified by MassLynx software. The values are the mean ± S.D. from three independent assays. Statistically significant differences are indicated; **, $p < 0.01$; t test.

severe reduction of 84% was observed toward C24:1-CoA, the main substrate of CERS2 (Fig. 4). These results demonstrate that the phosphorylation of HA-CERS2 is quite important for its enzymatic activity, and suggest that the activity of endogenous CERS2 is regulated by phosphorylation as well. The activities of CERS3–6 also seem to be regulated by phosphorylation, albeit modestly or weakly.

We further addressed whether the phosphorylation of endogenous CERS proteins in tissue is important for enzymatic activities. In the mouse brain, all *Cers* genes but *Cers3* are expressed (37). Brain sphingolipids consist mainly of C18 and C24 acyl-chains: *Cers1* synthesizes C18-Cer in neurons, whereas *Cers2* synthesizes C24-ceramides in oligodendrocytes (37, 38). Phosphorylation sites in the C-terminal regions are mostly conserved between mouse *Cers2–6* and human *CERS2–6* (Fig. 1). We prepared total membrane fractions from the mouse brain, treated them with or without λPPase, and measured ceramide synthase activities toward various acyl-CoAs. Treatment with λPPase reduced total ceramide synthase activity toward C16:0-CoA by 38%, C22:0-CoA by 88%, and C24:0-CoA by 85%; in contrast, activity toward C18:0-CoA was unchanged (Fig. 5). These results accord well with the observation that the HA-CERS2 protein, which exhibits activity toward C22/C24-CoAs, is highly dependent on phosphorylation (Fig. 4), and suggest that the activity of endogenous *Cers2* is regulated by phosphorylation in the mouse brain. Reduction in the activity toward C16:0-CoA may reflect a net effect of *Cers5* and *Cers6* dephosphorylation, although the relative contribution of each isozyme cannot be estimated.

CERS2–6 Phosphorylation in the C-terminal Region Is Required for Changes in Cellular Ceramide Composition—To examine the impact of CERS phosphorylation in the C-terminal region on cellular ceramide composition, we analyzed the distribution of ceramides having different acyl-chain compositions in cells expressing WT HA-CERS1–6 or MT HA-CERS2–6 using LC/MS. As expected from the known substrate

specificities of CERS isozymes (15), expression of each WT HA-CERS induced a characteristic shift in ceramide composition distinct from the composition of the control (Fig. 6). Expression of WT HA-CERS1 increased the level of C18:0-ceramide, whereas it reduced the levels of other species including C16:0-ceramide, C22:0-ceramide, and C24-ceramides. Expression of WT HA-CERS2 mainly increased the levels of VLC-ceramides including C22-ceramides and C24:1-ceramide, whereas it reduced the levels of C16:0-ceramide and C18:0-ceramide. Expression of WT HA-CERS3 increased the levels of C26:0-ceramide (the ULC-ceramide) as well as those of C18:0-ceramide, C20:0-ceramide, and C24:0-ceramide, whereas it reduced the level of C16:0-ceramide. These results are consistent with its broad substrate specificity reported in a previous study (39). Expression of WT HA-CERS4 increased the levels of C18-C22-ceramides, whereas it reduced the levels of C16:0-ceramide and C24-ceramides. WT HA-CERS5 and -6 had similar effects on ceramide composition: an increased level of C16:0-ceramide and decreased levels of C18:0-ceramide, C22:0-ceramide, and C24-ceramides. In contrast, MT HA-CERS2–6 caused little or no changes in ceramide composition compared with the control distribution. These results suggest that CERS phosphorylation in the C-terminal region is essential for efficient ceramide synthesis in cells, and that this phosphorylation has no apparent effect on each specificity of the isozyme for acyl-CoAs of certain defined chain lengths.

CERS2–6 Phosphorylation in the C-terminal Region Positively Regulates Enzymatic Activity—We examined whether the phosphorylation of CERS2–6 in their C-terminal regions regulates their enzymatic activities. We performed an *in vitro* ceramide synthase assay to compare the activities of each isozyme between their WT and MT variants. The activity of each MT HA-CERS was significantly reduced compared with that of its corresponding WT HA-CERS: HA-CERS2 (4A) by 35%, HA-CERS3 (S340A) by 10%, HA-CERS4 (4A) by 53%, HA-CERS5 (4A) by 27%, and HA-CERS6 (4A) by 10% (Fig. 7A). These results are essentially consistent with those of treating WT HA-CERS2–6 with λPPase (Fig. 4); however, the reductions were more severe for WT HA-CERS2–6 treated with λPPase than for MT HA-CERS2–6 (Figs. 4 and 7). These differences may have arisen from the pretreatment of WT HA-CERS2–6 with or without λPPase: the pretreatment changes the final buffer composition in the subsequent *in vitro* ceramide synthases assay and may partially inactivate ceramide synthases during incubation.

We next evaluated the contributions of individual residues in the C-terminal phosphorylation sites to the enzymatic activity of *Cers2*. We chose *Cers2* for further, detailed analyses, because loss of phosphorylation caused the most striking effects on the activity of *Cers2* among *Cers* isozymes (Figs. 4–6A). To do so, we expressed mouse HA-*Cers2* WT and five MT variants, in which Ser-341, Thr-346, Ser-348, Ser-349, or all four residues were substituted with Ala, separately in HEK 293T cells and performed an *in vitro* ceramide synthase assay. As expected, HA-*Cers2* (4A) was the most severely affected MT variant, with its activity reduced by 62% compared with WT HA-*Cers2* (Fig. 7B). Three of the four single mutation MT variants exhibited significantly reduced activities: in the order of severest to mild-
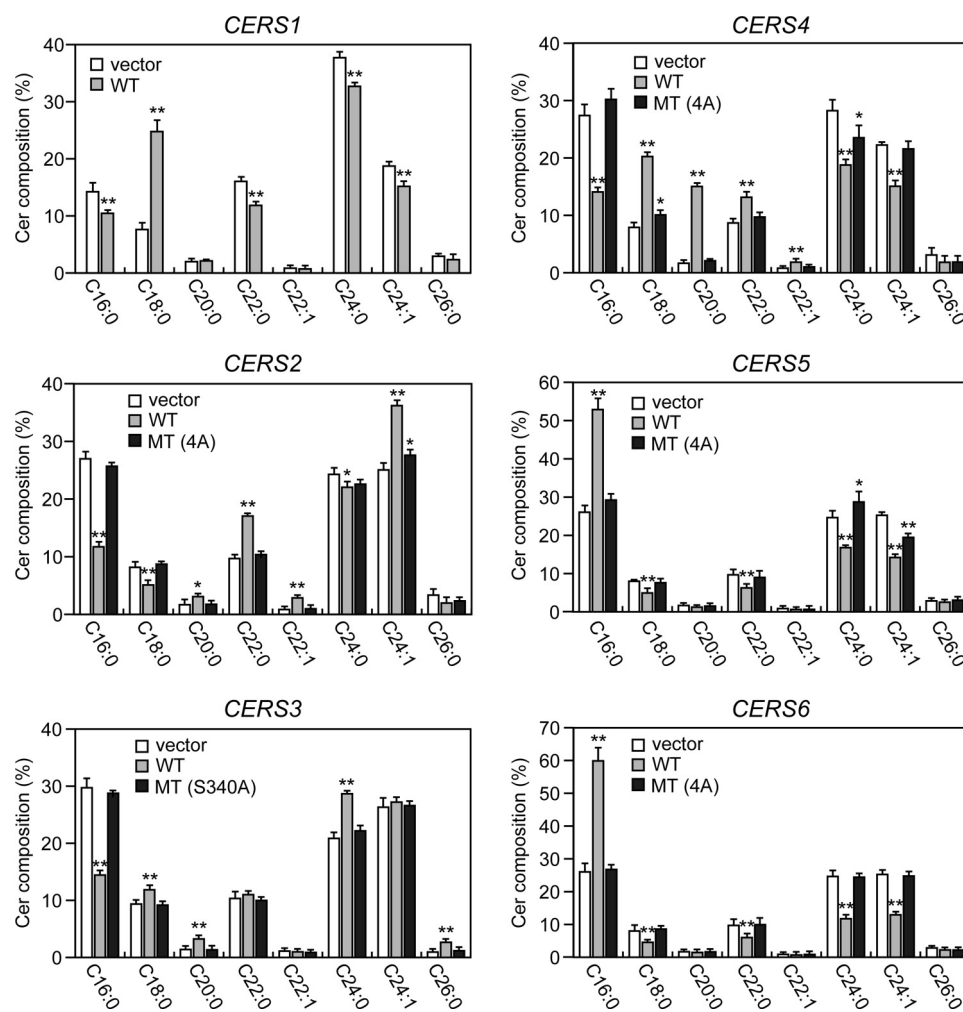
FIGURE 6. **Phosphorylation is required for CERS2–6 to function in cells.** HEK 293T cells were transfected with a vector or a plasmid encoding WT HA-CERS1–6 or MT HA-CERS2–6, as indicated. Twenty-four hours after transfection, lipids were extracted, and ceramide species were analyzed by a Xevo TQ-S LC/MS system and quantified by MassLynx software. The values represent the percent of each ceramide species relative to total ceramides, and are the mean ± S.D. from three independent experiments. Statistically significant differences are indicated; *, $p < 0.05$; **, $p < 0.01$; t test.

est, Cers2 (S341A), Cers2 (T346A), and Cers2 (S348A) (Fig. 7B). We observed by SDS-PAGE/immunoblot analysis that the electrophoretic mobility of each MT variant was clearly different from that of the WT protein, except for HA-Cers2 (S348A) (Fig. 7C). The S349A mutation did not affect enzymatic activity, yet induced the most obvious mobility shift among single mutation MT variants (Fig. 7C). Thus, there is no apparent correlation between the effects of mutation on enzymatic activity and any resultant shifts in mobility.

CERS2 Phosphorylation Regulates V_{max} and Affinities toward Sphingosine and Acyl-CoA Substrates—To examine how the activity of CERS2 is regulated by phosphorylation, we performed kinetic analyses of WT HA-CERS2 enzymes treated with or without λPPase. Kinetic analysis was performed by changing the concentration of one substrate while fixing the concentration of the other at a near saturation level in a ceramide synthase assay. K_m and V_{max} values were estimated by fitting the data to the Michaelis-Menten equation by nonlinear regression analysis. We found that phosphatase treatment severely reduced its V_{max} values by 84 or 94% compared with those of untreated controls (from 0.51 to 0.08 pmol/min/μg for sphingosine and from 0.76 to 0.04 pmol/min/μg for C24:1-

CoA) (Fig. 8, A and B). The phosphatase treatment increased its K_m value toward sphingosine to 7.70 μM from 1.07 μM for the untreated control (Fig. 8A). In contrast, the K_m value toward C24:1-CoA was reduced to 5.46 μM from 62.9 μM for the untreated control (Fig. 8B). These results demonstrate that the phosphorylation of HA-CERS2 in the C-terminal region increases its activity primarily by decreasing the V_{max} value of the associated reaction.

Discussion

In the present study, we demonstrated that mammalian ceramide synthases CERS2–6 are phosphorylated at their C-terminal regions (Fig. 2). We further identified CK2 as a protein kinase that phosphorylates mammalian ceramide synthases: specifically, CERS2, -4, -5, and -6 (Fig. 3). As reported recently, the catalytic components of yeast ceramide synthases, Lac1 and Lag1, are also phosphorylated by CK2 at their C-terminal regions (27), suggesting that the CK2-dependent phosphorylation of CERS is an evolutionarily conserved mechanism for the regulation of ceramide synthesis. In addition to their C-terminal regions, yeast Lac1 and Lag1 are phosphorylated at their N-terminal regions by the ortholog of mammalian SGK1
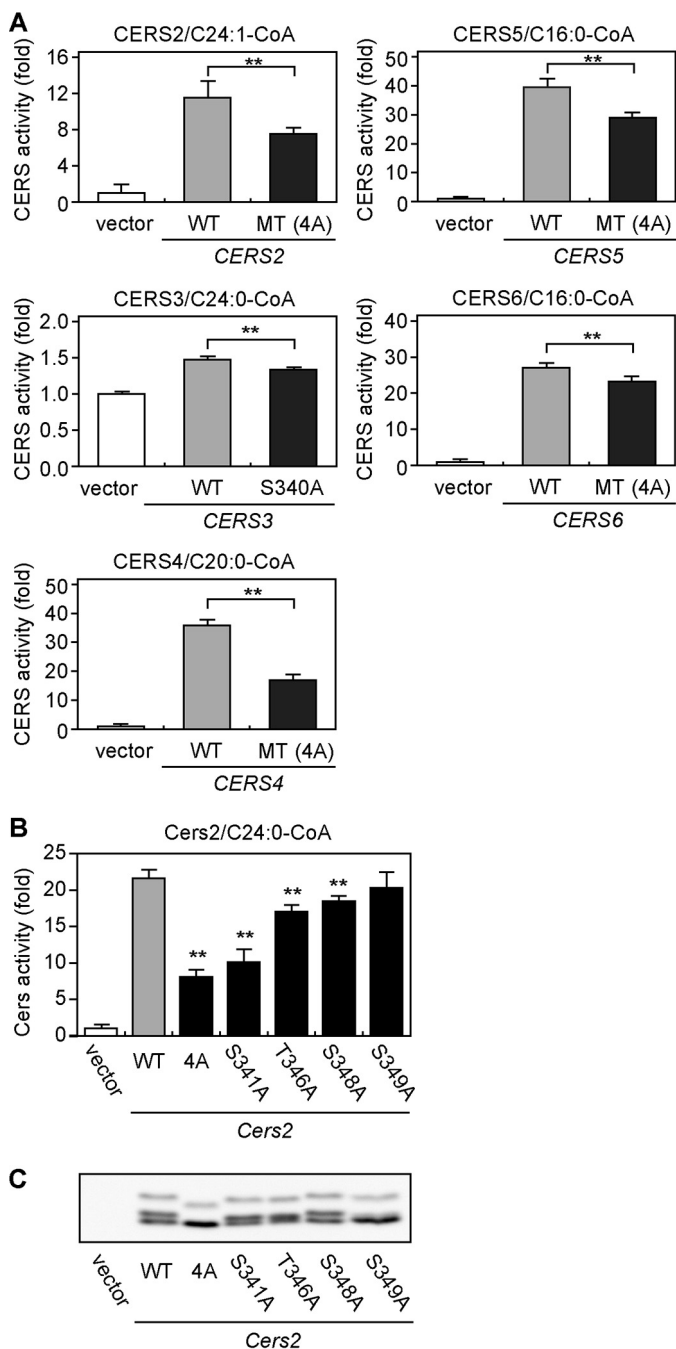
FIGURE 7. **Mutations in phosphorylation sites decrease enzymatic activity of CERS isozymes.** *A*, HEK 293T cells were transfected with a vector or a plasmid encoding WT HA-CERS1–6 or MT HA-CERS2–6, as indicated. *B* and *C*, HEK 293T cells were transfected with a vector or a plasmid encoding mouse WT HA-Cers2 or MT HA-Cers2, as indicated. *A* and *B*, total membrane fractions (10 μg of protein) prepared from the transfected cells were incubated with 5 μM deuterium-labeled sphingosine and 25 μM of the indicated acyl-CoA at 37 °C for 30 min. Lipids were extracted, and deuterium-labeled ceramides were analyzed by a Xevo TQ-S LC/MS system and quantified by MassLynx software. The values represent the activity of each CERS relative to that of the vector sample, and are the mean ± S.D. from three independent assays. Statistically significant differences in the activities between WT and MT are indicated; **, $p < 0.01$; *t* test. *C*, total membrane fractions (10 μg of protein) prepared from the transfected cells were separated by SDS-PAGE and subjected to immunoblotting with anti-HA antibodies.

(serum/glucocorticoid-regulated kinase 1) kinase Ypk1, which is activated by TORC2 (28). However, no consensus SGK1 phosphorylation motif could be found anywhere in the sequences
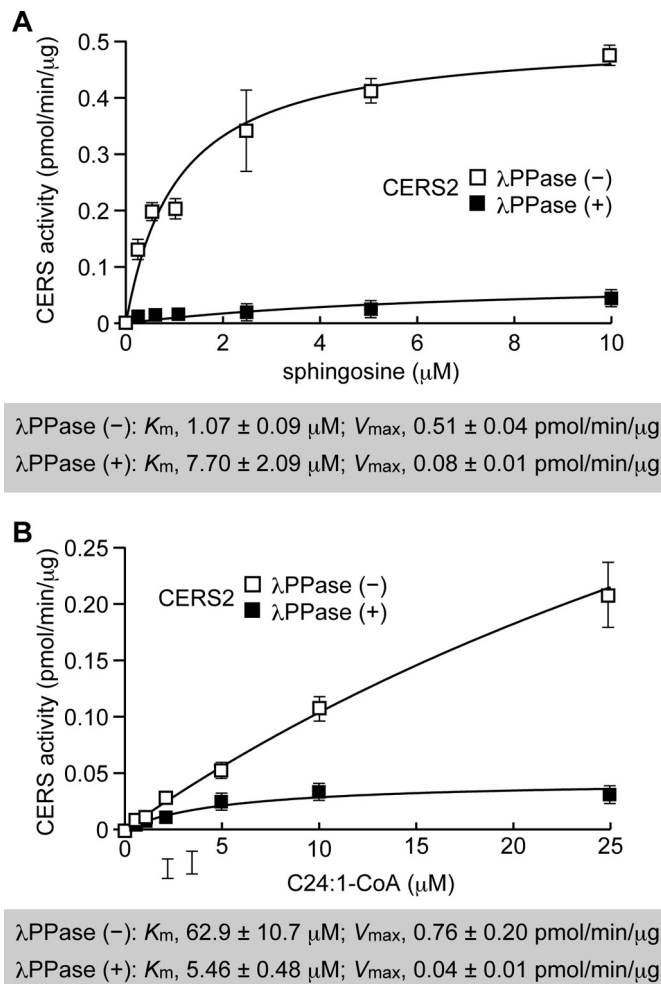

FIGURE 8. **Phosphorylation of CERS2 increases its V_{max} and regulates its affinities toward sphingosine and acyl-CoA substrates differently.** HEK 293T cells were transfected with a plasmid encoding WT HA-CERS2. Total membrane fractions (5 μg of protein) prepared from the transfected cells were treated with or without λPPase at 30 °C for 1 h, followed by incubation with the indicated concentrations of deuterium-labeled sphingosine and 25 μM of C24:1-CoA (*A*), or 5 μM deuterium-labeled sphingosine and the indicated concentrations of C24:1-CoA (*B*), at 37 °C for 30 min. Lipids were extracted, and deuterium-labeled ceramides were analyzed by a Xevo TQ-S LC/MS system and quantified by MassLynx software. The values represent the activity of each CERS, and are the mean ± S.D. from three independent measurements. The K_m and V_{max} values were estimated by fitting the data to the Michaelis-Menten equation by nonlinear regression analysis using ImageJ software.

for CERS1–6 (*i.e.* R*XRXX*(S/T)-Φ, where R stands for arginine, *X* for any amino acid, S for serine, T for threonine, and Φ for a hydrophobic amino acid), and we did not observe any further shift in the electrophoretic mobility of MT HA-CERS2–6 upon dephosphorylation by λPPase treatment (Fig. 2). The N-terminal regions of Lac1 and Lag1 face the cytosolic side of the endoplasmic reticulum and are subject to phosphorylation (28), whereas the N-terminal regions of mammalian CERS proteins are likely exposed to the lumen of the endoplasmic reticulum, as demonstrated by the *N*-glycosylation of CERS2, -5, and -6 in these regions (14). Therefore, we conclude that residues in the C-terminal region are the predominant phosphorylation sites in mammalian CERS2–6 proteins.

We demonstrated that the C-terminal regions of WT HA-CERS2, -4, -5, and -6 are phosphorylated by CK2 (Fig. 3). CK2 is

a highly pleiotropic, constitutively active Ser/Thr kinase that is responsible for catalyzing almost one-fourth of the known phosphoproteome (33). The expression level and activity of CK2 are elevated in many cancers originating from diverse tissues (40). CK2 exhibits cell-proliferative and anti-apoptotic properties, and is thus attracting increasing attention as a promising target for cancer treatment (34, 40). CK2 inhibitors such as CX-4945 are expected to decrease ceramide levels by inhibiting CERS phosphorylation. On the other hand, many studies have demonstrated that ceramides promote apoptosis by activating pro-death pathways or inhibiting pro-survival pathways (5). Thus, in the context of cell death induction, it seems that the inhibition of CERS phosphorylation by a CK2 inhibitor would exert an opposite, undesirable effect. Further work is necessary to clarify the role of ceramide and CERS phosphorylation in a CK2-dependent promotion of cell proliferation and counteraction of apoptosis in cancer.

Dephosphorylation exerted different effects on the activities of WT HA-CERS2–6 among isozymes (Fig. 4). The activity of HA-CERS2 highly depended on phosphorylation, and this regulation seems to apply similarly to endogenous CERS2 in HEK 293T (Fig. 4) and Cers2 in the mouse brain (Fig. 5). The kinetic analysis demonstrated that the phosphorylation of HA-CERS2 affects four parameters, namely its V_{max} values and K_m values toward sphingosine and acyl-CoA, severely reducing the V_{max} values in particular. The phosphorylation of CERS2 increased its affinity toward sphingosine (~7-fold decrease in K_m) while decreasing it toward C24:1-CoA (~12-fold increase in K_m). The C-terminal regions of CERS2–6 contain multiple acidic, Glu and Asp residues, and become further acidic by phosphorylation. These acidic C-terminal regions may bind to the positively charged amino group of the long-chain base and hold the molecule for effective catalysis, whereas they may repel C22/C24-CoAs through the negatively charged CoA moiety. Thus, the phosphorylation of CERS2 enables effective ceramide synthesis when the ratio of sphingosine to C22/C24-CoAs concentrations is low.

In contrast to HA-CERS2, the activities of HA-CERS3–6 were modestly or mildly reduced by λPPase treatment (Fig. 4). Their ceramide synthase assays were performed in the presence of sphingosine and acyl-CoA substrates at near-saturation levels, and therefore the activities measured were essentially their respective V_{max} values. It is possible that the phosphorylation affects V_{max} and K_m values differently in an isozyme-specific manner. Further kinetic analyses are necessary to clarify the impact of the phosphorylation of CERS3–6 on these parameters.

Despite *in vitro* activity remaining for MT HA-CERS2–6 compared with controls (Fig. 7), MT HA-CERS2–6 caused little or no changes in ceramide composition when expressed in cells, and behaved essentially as loss of activity mutants (Fig. 6). This apparent discrepancy may be explained by the low cellular concentration of long-chain bases, whose synthesis is rate-limiting for sphingolipid synthesis. Increasing CERS affinity toward long-chain bases by phosphorylation may be required for effective ceramide synthesis in cells. Alternatively, the discrepancy may be due to differences in accessibility to substrates between the *in vitro* ceramide synthase assay and the intracellular environment. The *in vitro* ceramide synthase assay mixture contains 0.1% digitonin as detergent, which may increase the solubility of substrates, facilitate the accessibility of substrates to membrane-embedded CERS, or modulate the conformation of CERS in an open state. These effects may bypass the necessity of CERS phosphorylation. In cells, CERS proteins may have rather limited access to substrates, or unphosphorylated CERS proteins may be in a closed state, and the phosphorylation could convert them into an open state to allow access to the substrates. The kinetic data demonstrating that phosphorylation of HA-CERS2 increases its affinity toward sphingosine as well as its V_{max} value may be in part consistent with this hypothesis.

CERS1 contains no potential phosphorylation sites in the C-terminal region, and treatment of CERS1 with λPPase did not induce any appreciable shift in electrophoretic mobility. Moreover, the treatment of mouse brain membrane fractions with λPPase did not affect activity toward C18:0-CoA, the preferred substrate of CERS1. However, it remains possible that CERS1 is phosphorylated in other cells or tissues, or under particular conditions. Indeed, it has been reported that CERS1 is phosphorylated under the activation of the protein kinase C pathway in response to treatment with 12-*O*-tetradecanoyl-phorbol-13 acetate (41).

Hyperactivation of CERS by phosphorylation may worsen the condition of diseases in which the levels of global or particular sphingolipid species are elevated. For example, CERS6-dependent elevation of C16-ceramide is associated with obesity and insulin resistance (42), and mutations in the *ASAH1* gene, which encodes acid ceramidase, cause Farber disease due to accumulation of ceramides in lysosomes (4, 43). Reducing ceramide synthesis by the inhibition of CERS phosphorylation may be a potential option to treat such diseases. CX-4945, a selective small-molecule CK2 inhibitor currently undergoing clinical trials for cancer treatment (34), may limit the accumulation of sphingolipids without the production of toxic metabolites such as *N*-acyl-fumonisin B_1, an undesirable byproduct of treatment with the CERS inhibitor fumonisin B_1 (44).

References

1. Breiden, B., and Sandhoff, K. (2014) The role of sphingolipid metabolism in cutaneous permeability barrier formation. *Biochim. Biophys. Acta* **1841,** 441–452
2. Kihara, A., Mitsutake, S., Mizutani, Y., and Igarashi, Y. (2007) Metabolism and biological functions of two phosphorylated sphingolipids, sphingosine 1-phosphate and ceramide 1-phosphate. *Prog. Lipid Res.* **46,** 126–144
3. Mendelson, K., Evans, T., and Hla, T. (2014) Sphingosine 1-phosphate signalling. *Development* **141,** 5–9
4. Schulze, H., and Sandhoff, K. (2014) Sphingolipids and lysosomal pathologies. *Biochim. Biophys. Acta* **1841,** 799–810
5. Truman, J. P., García-Barros, M., Obeid, L. M., and Hannun, Y. A. (2014) Evolving concepts in cancer therapy through targeting sphingolipid metabolism. *Biochim. Biophys. Acta* **1841,** 1174–1188
6. Turpin, S. M., Nicholls, H. T., Willmes, D. M., Mourier, A., Brodesser, S., Wunderlich, C. M., Mauer, J., Xu, E., Hammerschmidt, P., Brönneke, H. S., Trifunovic, A., LoSasso, G., Wunderlich, F. T., Kornfeld, J. W., Blüher, M.,

Krönke, M., and Brüning, J. C. (2014) Obesity-induced CerS6-dependent $C_{16:0}$ ceramide production promotes weight gain and glucose intolerance. *Cell Metab.* **20,** 678–686

7. Vanni, N., Fruscione, F., Ferlazzo, E., Striano, P., Robbiano, A., Traverso, M., Sander, T., Falace, A., Gazzerro, E., Bramanti, P., Bielawski, J., Fassio, A., Minetti, C., Genton, P., and Zara, F. (2014) Impairment of ceramide synthesis causes a novel progressive myoclonus epilepsy. *Ann. Neurol.* **76,** 206–212

8. Kihara, A. (2014) Sphingosine 1-phosphate is a key metabolite linking sphingolipids to glycerophospholipids. *Biochim. Biophys. Acta* **1841,** 766–772

9. Mullen, T. D., Hannun, Y. A., and Obeid, L. M. (2012) Ceramide synthases at the centre of sphingolipid metabolism and biology. *Biochem. J.* **441,** 789–802

10. Nakahara, K., Ohkuni, A., Kitamura, T., Abe, K., Naganuma, T., Ohno, Y., Zoeller, R. A., and Kihara, A. (2012) The Sjögren-Larsson syndrome gene encodes a hexadecenal dehydrogenase of the sphingosine 1-phosphate degradation pathway. *Mol. Cell* **46,** 461–471

11. Kihara, A. (2012) Very long-chain fatty acids: elongation, physiology and related disorders. *J. Biochem.* **152,** 387–395

12. Sassa, T., and Kihara, A. (2014) Metabolism of very-long-chain fatty acids: genes and pathophysiology. *Biomol. Ther. (Seoul)* **22,** 83–92

13. Sassa, T., Ohno, Y., Suzuki, S., Nomura, T., Nishioka, C., Kashiwagi, T., Hirayama, T., Akiyama, M., Taguchi, R., Shimizu, H., Itohara, S., and Kihara, A. (2013) Impaired epidermal permeability barrier in mice lacking *Elovl1*, the gene responsible for very-long-chain fatty acid production. *Mol. Cell. Biol.* **33,** 2787–2796

14. Mizutani, Y., Kihara, A., and Igarashi, Y. (2005) Mammalian Lass6 and its related family members regulate synthesis of specific ceramides. *Biochem. J.* **390,** 263–271

15. Mizutani, Y., Mitsutake, S., Tsuji, K., Kihara, A., and Igarashi, Y. (2009) Ceramide biosynthesis in keratinocyte and its role in skin function. *Biochimie* **91,** 784–790

16. Park, J. W., Park, W. J., and Futerman, A. H. (2014) Ceramide synthases as potential targets for therapeutic intervention in human diseases. *Biochim. Biophys. Acta* **1841,** 671–681

17. Mesicek, J., Lee, H., Feldman, T., Jiang, X., Skobeleva, A., Berdyshev, E. V., Haimovitz-Friedman, A., Fuks, Z., and Kolesnick, R. (2010) Ceramide synthases 2, 5, and 6 confer distinct roles in radiation-induced apoptosis in HeLa cells. *Cell. Signal.* **22,** 1300–1307

18. Sassa, T., Suto, S., Okayasu, Y., and Kihara, A. (2012) A shift in sphingolipid composition from C24 to C16 increases susceptibility to apoptosis in HeLa cells. *Biochim. Biophys. Acta* **1821,** 1031–1037

19. Atilla-Gokcumen, G. E., Muro, E., Relat-Goberna, J., Sasse, S., Bedigian, A., Coughlin, M. L., Garcia-Manyes, S., and Eggert, U. S. (2014) Dividing cells regulate their lipid composition and localization. *Cell* **156,** 428–439

20. Ginkel, C., Hartmann, D., vom Dorp, K., Zlomuzica, A., Farwanah, H., Eckhardt, M., Sandhoff, R., Degen, J., Rabionet, M., Dere, E., Dörmann, P., Sandhoff, K., and Willecke, K. (2012) Ablation of neuronal ceramide synthase 1 in mice decreases ganglioside levels and expression of myelin-associated glycoprotein in oligodendrocytes. *J. Biol. Chem.* **287,** 41888–41902

21. Zhao, L., Spassieva, S. D., Jucius, T. J., Shultz, L. D., Shick, H. E., Macklin, W. B., Hannun, Y. A., Obeid, L. M., and Ackerman, S. L. (2011) A deficiency of ceramide biosynthesis causes cerebellar purkinje cell neurodegeneration and lipofuscin accumulation. *PLoS Genet.* **7,** e1002063

22. Jennemann, R., Rabionet, M., Gorgas, K., Epstein, S., Dalpke, A., Rothermel, U., Bayerle, A., van der Hoeven, F., Imgrund, S., Kirsch, J., Nickel, W., Willecke, K., Riezman, H., Gröne, H. J., and Sandhoff, R. (2012) Loss of ceramide synthase 3 causes lethal skin barrier disruption. *Hum. Mol. Genet.* **21,** 586–608

23. Eckl, K. M., Tidhar, R., Thiele, H., Oji, V., Hausser, I., Brodesser, S., Preil, M. L., Onal-Akan, A., Stock, F., Müller, D., Becker, K., Casper, R., Nürnberg, G., Altmüller, J., Nürnberg, P., *et al.* (2013) Impaired epidermal ceramide synthesis causes autosomal recessive congenital ichthyosis and reveals the importance of ceramide acyl chain length. *J. Invest. Dermatol.* **133,** 2202–2211

24. Rabionet, M., Bayerle, A., Jennemann, R., Heid, H., Fuchser, J., Marsching,

C., Porubsky, S., Bolenz, C., Guillou, F., Gröne, H. J., Gorgas, K., and Sandhoff, R. (2015) Male meiotic cytokinesis requires ceramide synthase 3-dependent sphingolipids with unique membrane anchors. *Hum. Mol. Genet.* **24,** 4792–4808

25. Laviad, E. L., Kelly, S., Merrill, A. H., Jr., and Futerman, A. H. (2012) Modulation of ceramide synthase activity via dimerization. *J. Biol. Chem.* **287,** 21025–21033

26. Olsen, J. V., Blagoev, B., Gnad, F., Macek, B., Kumar, C., Mortensen, P., and Mann, M. (2006) Global, *in vivo*, and site-specific phosphorylation dynamics in signaling networks. *Cell* **127,** 635–648

27. Fresques, T., Niles, B., Aronova, S., Mogri, H., Rakhshandehroo, T., and Powers, T. (2015) Regulation of ceramide synthase by casein kinase 2-dependent phosphorylation in *Saccharomyces cerevisiae. J. Biol. Chem.* **290,** 1395–1403

28. Muir, A., Ramachandran, S., Roelants, F. M., Timmons, G., and Thorner, J. (2014) TORC2-dependent protein kinase Ypk1 phosphorylates ceramide synthase to stimulate synthesis of complex sphingolipids. *eLife* **3,** e03779

29. Ohno, Y., Nakamichi, S., Ohkuni, A., Kamiyama, N., Naoe, A., Tsujimura, H., Yokose, U., Sugiura, K., Ishikawa, J., Akiyama, M., and Kihara, A. (2015) Essential role of the cytochrome P450 CYP4F22 in the production of acylceramide, the key lipid for skin permeability barrier formation. *Proc. Natl. Acad. Sci. U.S.A.* **112,** 7707–7712

30. Ohno, Y., Suto, S., Yamanaka, M., Mizutani, Y., Mitsutake, S., Igarashi, Y., Sassa, T., and Kihara, A. (2010) ELOVL1 production of C24 acyl-CoAs is linked to C24 sphingolipid synthesis. *Proc. Natl. Acad. Sci. U.S.A.* **107,** 18439–18444

31. Ikeda, M., Kanao, Y., Yamanaka, M., Sakuraba, H., Mizutani, Y., Igarashi, Y., and Kihara, A. (2008) Characterization of four mammalian 3-hydroxyacyl-CoA dehydratases involved in very long-chain fatty acid synthesis. *FEBS Lett.* **582,** 2435–2440

32. Kitamura, T., Takagi, S., Naganuma, T., and Kihara, A. (2015) Mouse aldehyde dehydrogenase ALDH3B2 is localized to lipid droplets via two C-terminal tryptophan residues and lipid modification. *Biochem. J.* **465,** 79–87

33. Venerando, A., Ruzzene, M., and Pinna, L. A. (2014) Casein kinase: the triple meaning of a misnomer. *Biochem. J.* **460,** 141–156

34. Chon, H. J., Bae, K. J., Lee, Y., and Kim, J. (2015) The casein kinase 2 inhibitor, CX-4945, as an anti-cancer drug in treatment of human hematological malignancies. *Front. Pharmacol.* **6,** 70

35. Ferguson, A. D., Sheth, P. R., Basso, A. D., Paliwal, S., Gray, K., Fischmann, T. O., and Le, H. V. (2011) Structural basis of CX-4945 binding to human protein kinase CK2. *FEBS Lett.* **585,** 104–110

36. Siddiqui-Jain, A., Drygin, D., Streiner, N., Chua, P., Pierre, F., O'Brien, S. E., Bliesath, J., Omori, M., Huser, N., Ho, C., Proffitt, C., Schwaebe, M. K., Ryckman, D. M., Rice, W. G., and Anderes, K. (2010) CX-4945, an orally bioavailable selective inhibitor of protein kinase CK2, inhibits prosurvival and angiogenic signaling and exhibits antitumor efficacy. *Cancer Res.* **70,** 10288–10298

37. Becker, I., Wang-Eckhardt, L., Yaghootfam, A., Gieselmann, V., and Eckhardt, M. (2008) Differential expression of (dihydro)ceramide synthases in mouse brain: oligodendrocyte-specific expression of CerS2/Lass2. *Histochem. Cell Biol.* **129,** 233–241

38. Sugimoto, M., Shimizu, Y., Yoshioka, T., Wakabayashi, M., Tanaka, Y., Higashino, K., Numata, Y., Sakai, S., Kihara, A., Igarashi, Y., and Kuge, Y. (2015) Histological analyses by matrix-assisted laser desorption/ionization-imaging mass spectrometry reveal differential localization of sphingomyelin molecular species regulated by particular ceramide synthase in mouse brains. *Biochim. Biophys. Acta* **1851,** 1554–1565

39. Mizutani, Y., Kihara, A., and Igarashi, Y. (2006) LASS3 (longevity assurance homologue 3) is a mainly testis-specific (dihydro)ceramide synthase with relatively broad substrate specificity. *Biochem. J.* **398,** 531–538

40. Ruzzene, M., and Pinna, L. A. (2010) Addiction to protein kinase CK2: a common denominator of diverse cancer cells? *Biochim. Biophys. Acta* **1804,** 499–504

41. Sridevi, P., Alexander, H., Laviad, E. L., Pewzner-Jung, Y., Hannink, M., Futerman, A. H., and Alexander, S. (2009) Ceramide synthase 1 is regulated by proteasomal mediated turnover. *Biochim. Biophys. Acta* **1793,**

1218–1227

42. Raichur, S., Wang, S. T., Chan, P. W., Li, Y., Ching, J., Chaurasia, B., Chaurasia, B., Dogra, S., Öhman, M. K., Takeda, K., Sugii, S., Pewzner-Jung, Y., Futerman, A. H., and Summers, S. A. (2014) CerS2 haploinsufficiency inhibits β-oxidation and confers susceptibility to diet-induced steatohepatitis and insulin resistance. *Cell Metab.* **20,** 687–695

43. Gangoiti, P., Camacho, L., Arana, L., Ouro, A., Granado, M. H., Brizuela, L., Casas, J., Fabriás, G., Abad, J. L., Delgado, A., and Gómez-Muñoz, A.

(2010) Control of metabolism and signaling of simple bioactive sphingolipids: implications in disease. *Prog. Lipid Res.* **49,** 316–334

44. Harrer, H., Laviad, E. L., Humpf, H. U., and Futerman, A. H. (2013) Identification of *N*-acyl-fumonisin B1 as new cytotoxic metabolites of fumonisin mycotoxins. *Mol. Nutr. Food Res.* **57,** 516–522

45. Winter, E., and Ponting, C. P. (2002) TRAM, LAG1 and CLN8: members of a novel family of lipid-sensing domains? *Trends Biochem. Sci.* **27,** 381–383